

Supporting Information

High-performance n-type Ta₄SiTe₄/polyvinylidene fluoride (PVDF)/graphdiyne organic-inorganic flexible thermoelectric composites

Sanyin Qu^{1#}, Chen Ming^{1#}, Pengfei Qiu^{1,2*}, Kunqi Xu¹, Qing Xu^{1,3}, Qin Yao¹, Ping Lu¹, Huarong Zeng¹, Xun Shi^{1,3*}, Lidong Chen^{1,3}

Details about the X_d calculation

The thickness of the fully depleted layer (X_d) in the Ta₄SiTe₄ and GDY interface can be calculated by the depletion approximation^[1]

$$X_d = \left(\frac{2\varepsilon\Delta V}{qN_d} \right)^{1/2},$$

where ε , ΔV , q , and N_d are the dielectric constant of Ta₄SiTe₄, the built-in potential in the interfacial area, the elementary charge, and the carrier concentration of Ta₄SiTe₄. ε is assumed to be $10\varepsilon_0$ for Ta₄SiTe₄, where ε_0 is permittivity of vacuum. ΔV equals to the difference in work functions between Ta₄SiTe₄ and GDY.

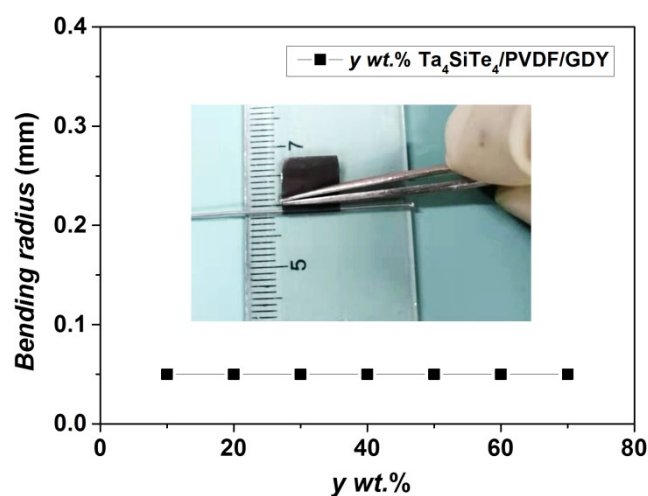


Fig. S1 Bending radius for the y wt.%PVDF/Ta₄SiTe₄/5.8 wt.%GDY composite films with different Ta₄SiTe₄ mass ratios. The inset shows the optical image of rolling the

composite film on a cylindrical object with $r = 0.05$ mm. This method was proposed by Liang et al. [2]

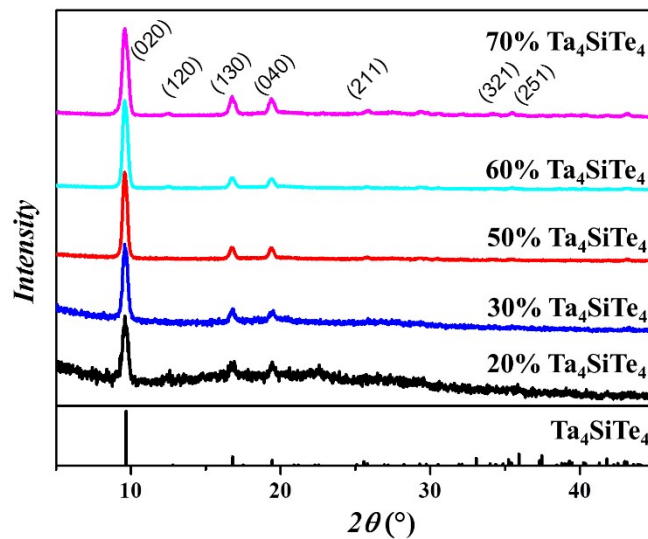


Fig. S2 X-ray diffraction patterns of the y wt.%PVDF/Ta₄SiTe₄/5.8 wt.%GDY composite films with different Ta₄SiTe₄ mass ratio.

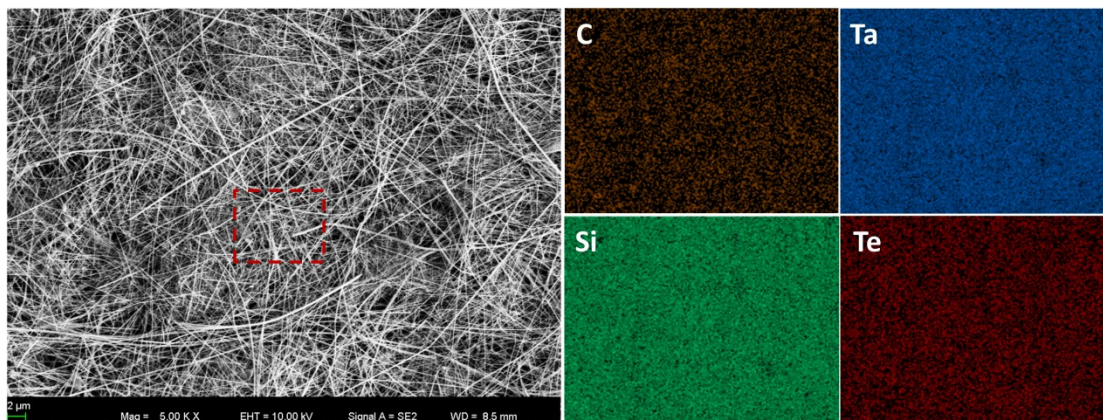


Fig. S3 SEM image of 50 wt.%Ta₄SiTe₄/PVDF/5.8 wt.%GDY composite film and the elemental mapping of Ta, Si, Te, and C.

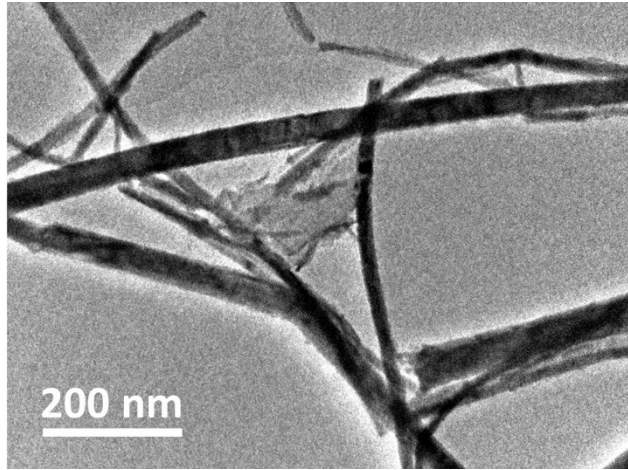


Fig. S4 Low-resolution TEM images of Ta₄SiTe₄/GDY composites.

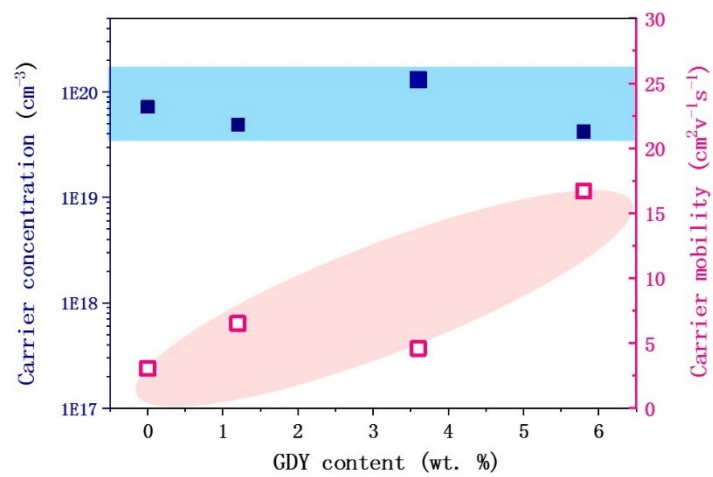


Fig. S5 Carrier concentration and carrier mobility of 50 wt.%PVDF/Ta₄SiTe₄/*x* wt.%GDY (*x* = 0, 1.2, 3.6, and 5.8) composite films.

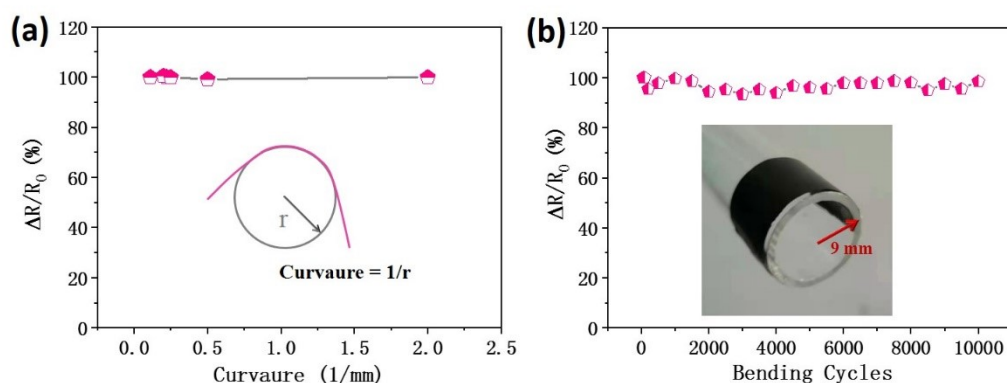


Fig. S6 (a) Relative resistance variation ($\Delta R/R_0$) as a function of various curvatures for 50 wt.% Ta₄SiTe₄/PVDF/5.8 wt.% GDY composite film. b) $\Delta R/R_0$ as a function of bending cycles over a curvature of 0.11 mm⁻¹ for 50 wt.% Ta₄SiTe₄/PVDF/5.8 wt.% GDY composite film. The resistance is almost unchanged after 10000 bending cycles.

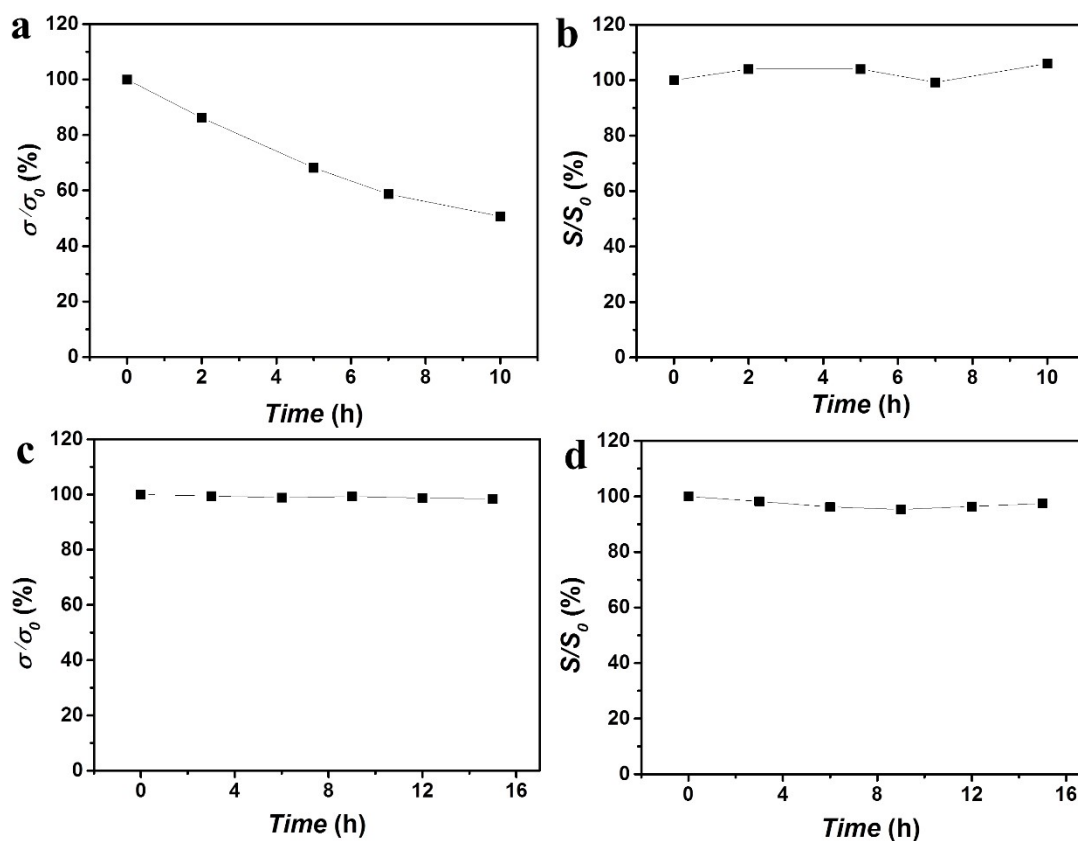


Fig. S7 Electrical conductivity and Seebeck coefficient variations of 50 wt.%PVDF/Ta₄SiTe₄/5.8 wt.%GDY composite film during the stability test (a-b) in air and (c-d) Argon atmosphere.

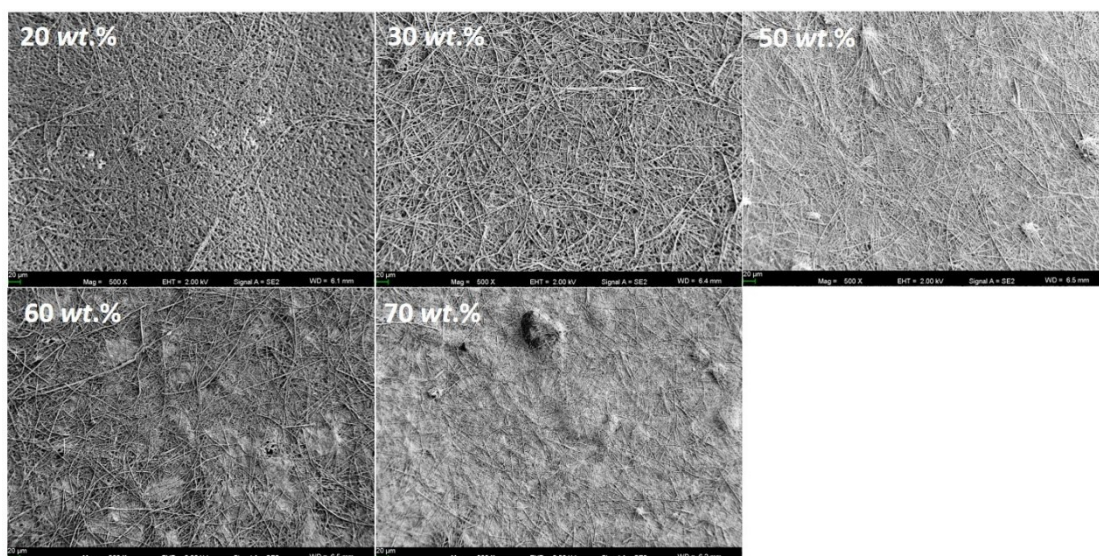


Fig. S8 SEM images of y wt.% Ta_4SiTe_4 /PVDF/5.8 wt.%GDY ($y = 20, 30, 50, 60,$ and 70) composite films.

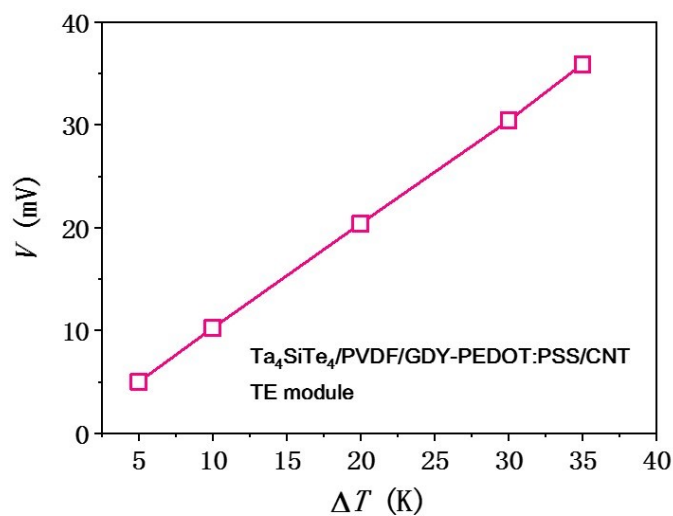


Fig. S9 Open voltage (V) as a function of temperature gradient (ΔT) for the prototype Ta_4SiTe_4 /PVDF/GDY-PEDOT:PSS/CNT TE module.

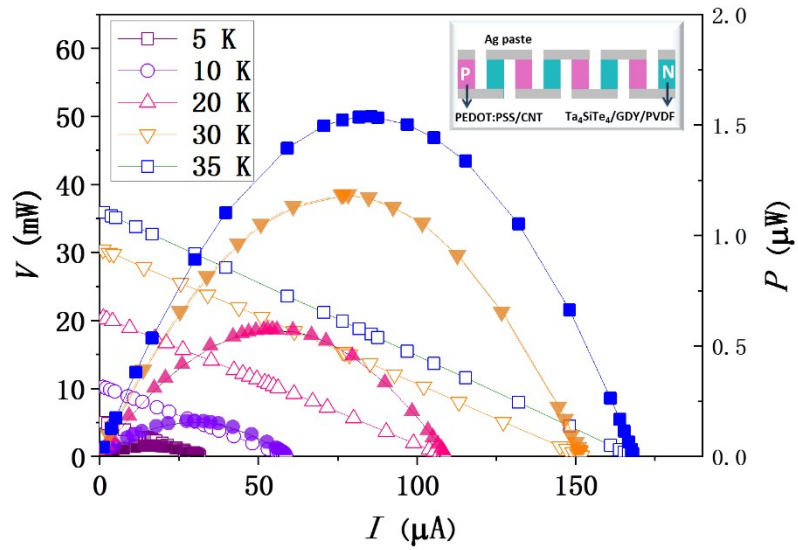


Fig. S10 Output voltage (V) and power (P) as a function of current (I) for prototype Ta₄SiTe₄/PVDF/GDY-PEDOT:PSS/CNT TE module under different operating temperatures. The inset shows the sketch map of the prototype module.

References

- [1] D. A. Neamen, *Semiconductor Physics and Devices, Basic Principles*, New York: The McGraw-Hill Companies, Inc.
- [2] L. R. Liang, C. Y. Gao, G. M. Chen, C-Y Guo, *J. Mater. Chem. C*, 2016, **4**, 526.